Journal of Mines, Metals and Fuels, *73(10): 3201-3214; 2025. DOI: 10.18311/jmmf/2025/49905*

Online ISSN : 0022-2755

Journal of Mines, Metals and Fuels

Contents available at: *www.informaticsjournals.co.in/index.php/jmmf*

Geotechnical Enhancement and Carbon Sequestration in Expansive Soils using Ground Granulated Blast Slag

H. N. Raghavendra[1], H. Likhitha[2], N. Muralidhar[3], T. P. Sanjeev[1] and Arunkumar Yadav[4*]

[1]Department of Civil Engineering, Dayananda Sagar College of Engineering, Bangalore - 560078, Karnataka, India
[2]Department of Civil Engineering, Global Academy of Technology, Bangalore - 560098, Karnataka, India
[3]Department of Civil Engineering, Malnad College of Engineering, Hassan - 573202, Karnataka, India
[4]Department of Civil Engineering, Manipal Institute of Technology, Bangalore - 575025, Karnataka, India; arunkumar.yadav@manipal.edu

Abstract

Expansive soils, characterised by high plasticity and susceptibility to moisture-induced volume changes, pose major challenges to infrastructure performance. This study investigates the use of Ground Granulated Blast furnace Slag (GGBS) as a soil stabiliser and a medium for CO_2 sequestration under accelerated carbonation conditions. Laboratory experiments with GGBS additions of 10%, 20%, and 30% showed marked improvements in soil behaviour. Unconfined Compressive Strength (UCS) increased notably, with 20% GGBS-treated soils initially reaching 2.32 kg/cm^2, though exposure to CO_2 over 24 h led to a gradual strength reduction to 0.69 kg/cm^2. Plasticity Index (PI) values decreased across all treatments, with the untreated soil dropping from 32 to 24.2, while the 30% GGBS mix showed a sharper initial decline from 22 to 16.29, stabilising at 21.1 after 24 h. CO_2 adsorption capacity was highest in the 30% GGBS samples, peaking at 36 mg/g before reducing to 25 mg/g, reflecting substantial carbonation potential. Machine learning models, including Random Forest and XGBoost, were employed to predict UCS, PI, and CO_2 uptake. Among them, XGBoost consistently achieved superior predictive accuracy across all variables and exposure conditions. These findings highlight the promising role of GGBS in sustainable soil stabilisation, offering both mechanical improvement and environmental benefits through carbon sequestration.

Major Findings: *The addition of GGBS significantly improves the geotechnical properties of expansive soils while enabling short-term CO_2 sequestration through accelerated carbonation. A 20% GGBS mix yields the highest initial strength, while 30% GGBS shows maximum CO_2 uptake (36 mg/g) and plasticity reduction. Machine learning models, especially XGBoost, effectively predict UCS, PI, and CO_2 adsorption with high accuracy, reinforcing the experimental trends.*

Keywords: *Black Cotton Soil, CO_2 Sequestration, GGBS, Machine Learning, Random Forest, XGBoost*

1.0 Introduction

Expansive soils, rich in clay minerals like montmorillonite, undergo significant volume changes with moisture variation, leading to structural damage in buildings, pavements, pipelines, and foundations[1,2]. Characterised by high specific surface area and cation exchange capacity, they pose a global geotechnical challenge, particularly in arid and semi-arid regions such as Australia, India, the US, and China[3]. In India, these soils—commonly known as Black Cotton soils—cover around 20% of the land[4], and have caused billions in structural damage worldwide[5,6].

**Author for correspondence*

Stabilisation of expansive soils often relies on additives capable of supplying sufficient calcium, with industrial by-products like fly ash, blast furnace slag, cement kiln dust, and limestone dust emerging as effective and low-cost alternatives[7-15]. These materials, rich in siliceous and calcareous components, also reduce greenhouse gas emissions by replacing traditional stabilisers. Conventional additives such as lime and cement, though effective, are produced through energy-intensive processes that emit significant CO_2, CH_4, and N_2O[16-19]. In India, fly ash and granulated blast furnace slag (GGBS) are the most abundantly generated industrial wastes, with annual outputs of approximately 170 and 15 million tonnes, respectively[20,21]. While fly ash is primarily used in cement, road construction, and brick manufacturing, GGBS serves mainly as a partial cement substitute. Despite their potential as soil stabilisers, their utilisation remains limited—58% for fly ash and 55% for GGBS—due to low pozzolanic reactivity[21,22]. Indian fly ash, derived from bituminous coal, contains less than 10% lime[23], whereas GGBS, a latent hydraulic binder rich in lime, requires activation to perform effectively[24]. Several studies[25-29] have explored the use of GGBS as a soil stabiliser, reporting slight modifications in Atterberg limits and improvements in compaction characteristics like Maximum Dry Density (MDD) and Optimum Moisture Content (OMC). However, enhancements in UCS were gradual due to the latent hydraulic nature of GGBS, which reacts slowly in water, forming an aluminosilicate layer that inhibits further hydration. To activate GGBS and accelerate strength gain, high-pH additives like cement and lime are commonly employed[30-33].

Furthermore, Carbon dioxide, a key greenhouse gas, contributes significantly to global warming by trapping heat in the atmosphere[34]. The escalating global energy demand, driven by rapid population growth and industrialisation, has significantly increased the reliance on fossil fuels, leading to an alarming rise in carbon dioxide (CO_2) emissions and intensifying the global warming crisis. The construction sector, in particular, has further exacerbated this issue through the extensive use of carbon-intensive materials such as Portland cement. In response, the scientific community has prioritised the development of advanced mitigation strategies to curb greenhouse gas emissions. Among these, Carbon Capture, Utilisation, and Storage (CCUS) have emerged as a pivotal technology, wherein CO_2 is sequestered from emission sources and permanently stored in deep geological formations. With growing global urgency to address climate change, governments are prioritising safe and economical methods to reduce atmospheric CO_2, among which mineral carbonation stands out as a promising approach for cutting industrial greenhouse gas emissions. As highlighted in the Intergovernmental Panel on Climate Change (IPCC) Sixth Assessment Report, 2021, CCUS plays a crucial role in achieving net-zero CO_2 emissions by 2050[35-38]. Complementarily, carbonation, a naturally occurring or induced chemical process involving the reaction of CO_2 with alkaline substances to form stable carbonates, bicarbonates, and carbonic acid, has gained attention as an effective CO_2 sequestration pathway[39-43]. Natural carbonation, synonymous with mineral weathering, further facilitates long-term atmospheric CO_2 removal through geochemical reactions with naturally occurring alkaline minerals[44].

Natural carbonation of basalt can sequester up to 94.15 kg of CO_2 per cubic meter, but its effectiveness is limited by the slow reaction rate caused by low atmospheric CO_2 concentrations (0.03%–0.06%)[45,46]. Accelerated carbonation, achieved by injecting high-purity CO_2 into alkaline materials, significantly boosts the formation of stable carbonates within hours, offering an effective method for CO_2 removal[47]. CO_2 removal technologies generally operate through two main pathways: reactions with naturally occurring minerals and those involving industrial alkaline wastes[47]. The former relies on calcium- or magnesium-rich materials like olivine and serpentine to form stable carbonates under controlled thermal and pressure conditions, though the process is often constrained by its high energy demands[46,48]. Alternatively, industrial by-products such as steel slag, blast furnace slag, and cement kiln dust offer a more direct and energy-efficient route, leveraging their inherent chemical reactivity without the need for extensive pre-treatment[49,50]. Various Carbon Dioxide Removal (CDR) methods have been proposed, including biological, physical, and chemical approaches. Biological methods involve plant-driven carbonation within plant-soil systems[51,52], while physical methods focus on capturing and storing CO_2 in geological formations or oceans[53-55]. The chemical method, which includes natural and accelerated carbonation processes, utilises reactions between CO_2 and silicate minerals like olivine to form carbonates[56,57]. Due to its lower energy requirements and

practical applicability, adsorption is one approach for post-combustion carbon capture[58]. Research is increasingly focused on enhancing this method using various adsorbents such as zeolites, alkaline solvents, activated carbon, and engineered biochar[59-62]. Clay minerals like montmorillonite and kaolinite offer potential for CO_2 adsorption due to their stability, though effectiveness varies with interlayer composition and treatment[63,64]. Acid-treated kaolinite shows improved adsorption over untreated forms[64]. Kaolinitic clays exhibit notable CO_2 selectivity over gases like methane and nitrogen, with adsorption capacities ranging from 0.13–0.15 mmol/g across 15–55°C, influenced by surface area and pore volume[65-67]. In comparison, montmorillonite shows lower but temperature-dependent adsorption, though most studies focus on pure clays, which may differ from natural clay mixtures[68]. Laboratory investigations have shown that CO_2 deposition can enhance soil stability by increasing compressive strength and reducing permeability, with its effectiveness influenced by factors such as soil type, flow rate, and exposure duration[69]. Further research on alkali-activated olivine revealed its potential as a sustainable soil stabiliser, where carbonation contributed to improved strength and microstructural development over time through the formation of carbonate minerals[70].

The study aims to explore the functionality of GGBS as a soil stabiliser and a medium for Carbon Dioxide (CO_2) sequestration through accelerated carbonation. It evaluates the influence of different GGBS dosages and CO_2 exposure durations on UCS, PI, and CO_2 adsorption capacity. Additionally, machine learning models, specifically Random Forest and XGBoost, are applied to predict these soil properties and assess their behaviour over time. This combined experimental and predictive approach provides a comprehensive understanding of both soil performance and its environmental benefits, offering a sustainable method for soil stabilisation and carbon management.

2.0 Materials and Methods

2.1 Soil Characteristics

The soil utilised in this investigation was black cotton soil, sourced from a depth of 1.5 meters at Belgaum, Karnataka, with the removal of topsoil to eliminate the influence of organic matter. Collected during excavation works, the sample underwent comprehensive laboratory characterisation to evaluate its geotechnical properties. Sieve analysis conducted as per IS 2720-Part 4 (1985)[71] indicated that 54% of the particles were finer than 75 µm, signifying a predominance of silt and clay-sized fractions. Hydrometer analysis confirmed a clay content of approximately 40 ± 2%. The Atterberg limits, determined following IS 2720-Part 5[72], revealed a liquid limit of 72% and a plastic limit of 40%, categorising the soil as fine-grained with high plasticity, as presented in Table 1.

Table 1. Properties of black soil

Properties	Value
Specific gravity	2.68
Moisture content	40 ~ 45%
Percentage of sand	46%
Percentage of silt and clay	54%
Liquid limit	72%
Plastic limit	40%
Classification	CH
Maximum dry density	1.36 g/cm^3
Optimum m/c	26%
Unconfined strength	1.61 kg/cm^2

2.2 Ground Granulated Slag

Steel industry by-products like slag require neutralisation for environmental safety. Depending on cooling methods, slag is classified as air-cooled blast furnace slag or granulated slag, the latter of which is finely ground to produce ground granulated blast furnace slag[73,74]. Table 2 presents the physical and chemical properties of GGBS. The specific surface area is 380 m^2/kg, and the calcium oxide content is in the range of 32-40 %, which contributes to its reactivity and suitability for soil stabilisation. Key components like silica (25–37 %) and alumina (9–15 %) support pozzolanic activity, while low loss on ignition (2.1%) indicates minimal volatile content.

2.3 Methodology

The oven-dried soil and various proportions of GGBS (0%, 10%, 20%, and 30% by weight) are added to create different treatment levels. After thoroughly mixing each soil-GGBS combination, water is added to achieve the optimum moisture content of the soil, followed by compaction in cylindrical molds to ensure uniform

Table 2. Properties of GGBS

Properties	Value
Physical	
Specific gravity	2.91
Specific surface area	380 m^2/kg
Loss of ignition (% wt)	2.1
Chemical (% wt)	
Silica	25-37
Aluminium oxide	9-15
Iron oxide	0.32-1.8
Calcium oxide	32-40
Magnesium oxide	0.11-0.67
Titanium oxide	-
Phosphorous	-
Sulphates	1-2.5
Alkali oxides	-

density. The samples are then cured for 7 days under controlled conditions (23±2°C and 50-60% relative humidity) to allow for initial stabilisation reactions. After curing, the samples are exposed to CO_2 in a controlled chamber with a constant CO_2 concentration (*e.g.*, 10%) and environmental conditions (25°C, 50-60% relative humidity). Natural carbonation is a slow process limited by the low concentration of atmospheric CO_2 (~0.04%). Therefore, accelerated carbonation is employed, as it offers a controlled environment with elevated CO_2 levels, enabling observable and quantifiable changes within shorter timeframes suitable for practical experimental analysis. Exposure times are set at 1, 3, 5, 7, and 24 h, with additional untreated control samples kept at ambient conditions to serve as a baseline. Several tests are performed on each treated and CO_2-exposed sample. UCS testing is conducted at each exposure period to assess strength characteristics from GGBS treatment and CO_2 exposure, while Atterberg limits tests determine changes in PI, indicating the effect of carbonation on soil workability. These tests provide insights into the soil's mechanical and plasticity characteristics. Further, CO_2 uptake is measured to assess carbonation levels using a colorimetric method or by measuring weight change before and after exposure. In parallel, a machine learning approach was employed to model and predict the behaviour of soil properties under varying conditions. The dataset generated from the experimental results, comprising variables such as GGBS content, exposure time, UCS, PI, and CO_2 uptake, was used to train two supervised regression models: Random Forest and XGBoost. These models were evaluated based on their ability to accurately predict soil responses across different treatment levels and exposure durations. Model performance was assessed using Root Mean Square Error (RMSE), and comparative analyses between actual and predicted values were conducted to validate their effectiveness.

3.0 Results and Discussions

3.1 Unconfined Strength

Figure 1 shows the effect of CO_2 exposure on the UCS of soil samples treated with varying amounts of GGBS over time. Untreated soil (B) experiences an initial sharp decrease in UCS from 1.61 at 0 hr to 0.46 at 5 h. However, its strength slightly rebounds to 0.6 at 7 h and stabilises at around 0.74 by 24 h. This initial drop is likely due to the formation of weak carbonic acid from CO_2, which temporarily softens the soil. Over time, a secondary reaction, carbonation, may take place where calcium compounds in the soil react with CO_2 to form stable calcium carbonate, explaining the slight rebound in strength as the soil begins to stabilise.

For soil treated with 10% GGBS (S1), the UCS also decreases from 1.91 at 0 hr to 0.58 at 5 hr, then stabilises with a small increase to 0.55 at 7 h and further to 0.71 by 24 h. GGBS has latent hydraulic properties and reacts slowly in the presence of moisture to form calcium-silicate-hydrate (C-S-H) compounds, which contribute to soil strength over time. Additionally, GGBS may participate in carbonation reactions, producing stable

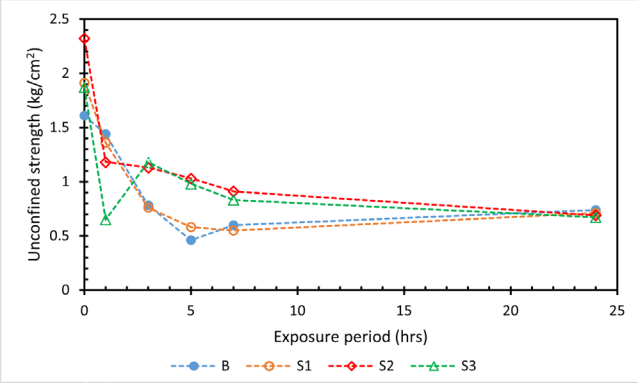


Figure 1. Variation of UCS at different exposure periods.

calcium carbonate phases that help regain strength after the initial decline. This gradual stabilisation suggests that 10% GGBS content supports the soil's ability to retain compressive strength under prolonged CO_2 exposure.

With 20% GGBS (S2), the UCS initially peaks at 2.32 kg/cm² due to effective hydraulic binding from the added slag. However, the strength steadily declines to 1.03 kg/cm² at 5 h and further to 0.69 kg/cm² by 24 h of CO_2 exposure. This reduction is attributed to increased reactivity with CO_2, which promotes both carbonation and hydration reactions. Despite this, the carbonation appears insufficient to form stable carbonate phases that can counteract the initial weakening. Additionally, excessive carbonation may lead to microstructural disruption, either through the formation of expansive reaction products or the densification of pore spaces, which inhibits further strength gain. As a result, the final UCS remains significantly lower than the initial value, indicating a diminishing return in mechanical performance at this GGBS content under accelerated carbonation.

In the case of soil treated with 30% GGBS (S3), the UCS first drops from 1.87 at 0 hr to 0.65 at 1 hr, then suddenly rises to 1.18 at 3 hrs, before gradually decreasing to 0.67 by 24 h. This can be attributed to the fact that rapid carbonation reactions temporarily enhance soil stability. However, with prolonged CO_2 exposure, the high GGBS content may lead to excessive carbonation, creating more porous zones and potentially disrupting the structure of hydration products, which results in a long-term decrease in UCS.

Initially, carbonation forms carbonic acid, which causes softening and a reduction in strength. However, over time, the precipitation of stable $CaCO_3$ enhances particle bonding and reduces porosity, leading to long-term strength recovery. While hydration reactions contribute to early strength development, carbonation can further improve strength through the formation of $CaCO_3$. Excessive carbonation, though, consumes $Ca(OH)_2$, disrupting ongoing hydration, particularly at higher GGBS dosages[75,76], resulting in a trade-off in overall strength development.

3.2 Plasticity Characteristics

Figure 2 illustrates the effect of CO_2 exposure on the PI of soils treated with different percentages of GGBS for different durations. For the untreated soil, B, the PI

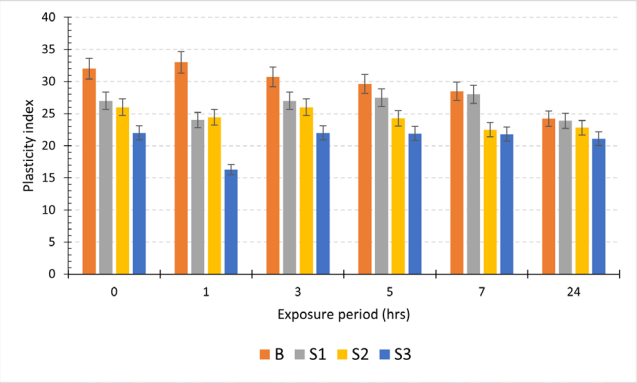


Figure 2. Plasticity vs exposure period.

initiates at 32 and gradually decreases to 24.2 after 24 h. This initial decrease is due to CO_2 interacting with minerals in the soil to form weak carbonic acid, which begins to slightly alter the soil structure. Over time, prolonged exposure to CO_2 promotes the formation of calcium carbonate[77] through natural carbonation, making the soil structure more stable and reducing its plasticity.

For the soil containing 10% GGBS, S1, PI is initially 27 and rapidly decreases to 24 after 1 h of CO_2 exposure. However, it increases slightly to 27 after 3 h before declining steadily to 23.9 after 24 h. The addition of 10% GGBS provides a source of calcium and alumina that promotes stabilisation. The initial decrease in PI is due to the formation of calcium carbonate, which reduces plasticity by flocculating clay particles. The slight increase at 3 h may be due to intermediate reactions between CO_2 and GGBS that temporarily affect plasticity. Thereafter, PI continues to decrease as carbonation further stabilises the soil structure.

For the soil treated with 20% GGBS, S2, PI starts at 26 and drops to 24.42 within 1 h, then shows little fluctuation before gradually decreasing to 22.8 by 24 h. This suggests that a higher GGBS content supports a stronger initial reaction, rapidly reducing PI as calcium carbonate forms, further stabilising the soil. The stability observed after 1 h indicates that 20% GGBS provides a balanced effect, with ongoing carbonation reducing plasticity over time and increasing the stability of the soil structure.

The 30% GGBS soil, S3, exhibits the lowest initial PI of 22, which declines sharply to 16.29 after 1 h of CO_2 exposure. The PI then reverts to 22 after 3 h and fluctuates slightly before settling at 21.1 after 24 h. The high GGBS content facilitates rapid carbonation, resulting in a steep initial drop in plasticity. The increase at 3 h may be due

to intermediate hydration reactions that temporarily affect the plasticity. After these reactions stabilise, the soil maintains a lower PI, indicating a significant improvement in long-term stability.

Thus, 10% GGBS dosage likely maintains optimal moisture–binder ratio, allowing effective hydration and carbonation without causing over-saturation or porosity, leading to better structural integrity.

3.3 CO_2 Adsorption

From Figure 3, sample B, the CO_2 uptake begins at 19 mg/g after 1 h, peaks at 29 mg/g at 3 h, and then gradually decreases, reaching 11 mg/g by 24 h. This initial increase can be attributed to natural minerals in the soil reacting with CO_2 to form weak carbonic acid. However, without GGBS to provide calcium, the carbonation potential is limited, and uptake decreases as reactions stabilise over time. In soil treated with 10% GGBS, S1, CO_2 uptake starts higher, at 25 mg/g, and peaks at 31 mg/g at 5 h before slowly declining to 14 mg/g by 24 h. The addition of GGBS introduces calcium, which reacts with CO_2 to form calcium carbonate, promoting carbonation. However, as reactive sites become saturated, the uptake rate slows, leading to a decline after the initial peak.

For soil with 20% GGBS, S2, CO_2 uptake increases from 32 mg/g to 34 mg/g after 5 h and then decreases to 25 mg/g after 24 h. The higher GGBS content provides more calcium, which supports a stronger and more sustained carbonation reaction compared to S1. After 5 h, the reaction sites become saturated, resulting in a slower decline in uptake, indicating more stable carbonation. The soil with 30% GGBS, S3, shows the highest CO_2 uptake, starting at 30 mg/g, peaking at 36 mg/g after 5 h, and gradually decreasing to 25 mg/g after 24 h. The high GGBS content allows for rapid and extensive carbonation due to the high availability of calcium. Although the uptake decreases slightly after 5 h, it remains relatively high, suggesting a robust, long-term carbonation potential.

3.4 Machine Learning Model

Recently, artificial intelligence has been increasingly applied to predict soil properties, showing strong performance and advantages. Studies have used various techniques, including logistic regression for fine-grained soils[78], SVM and its variants like AD-SVM and ICA-SVM for lateritic soils, with ICA-SVM outperforming

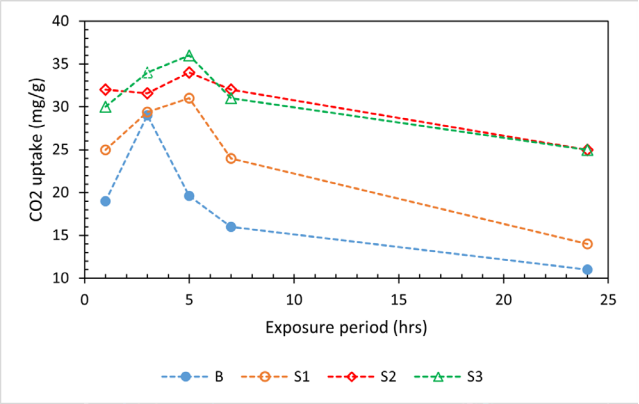


Figure 3. Adsorption of CO_2 at different periods.

others[79,80], and ANN models for predicting compaction and permeability, where MARS models proved most accurate for sandy soils[81-83]. ANN models have also been optimised using different hidden layers, neurons, and activation functions, with Tanh performing best[84], while GEP and MEP have been successfully used for expansive soils[85]. Feature importance analysis highlighted the role of liquid limit, plastic limit, and sand content in predicting optimum moisture content and maximum dry density[82,85].

3.4.1 Random Forest

Random Forest (RF), a bagging-based ensemble learning method, uses decision trees as its core units and combines their outputs through averaging or voting to improve prediction or classification accuracy (Figure 4). It integrates bagging and random feature selection during tree construction, where random subsets of features are used for node splitting, helping reduce tree correlation and enhance overall model performance[86].

The Random Forest (RF) algorithm operates by repeatedly sampling subsets of data and features from the original dataset to build multiple decision trees. At each node, the best feature from the selected subset is used for splitting, and this process is repeated across all trees. For classification tasks, the final output is determined through majority voting, while for regression, it's based on the average of the trees' predictions. Known for its high accuracy, robustness against overfitting, parallel training capability, flexibility, and user- user-friendliness, RF has become a widely adopted tool across various fields for solving both classification and prediction challenges[87].

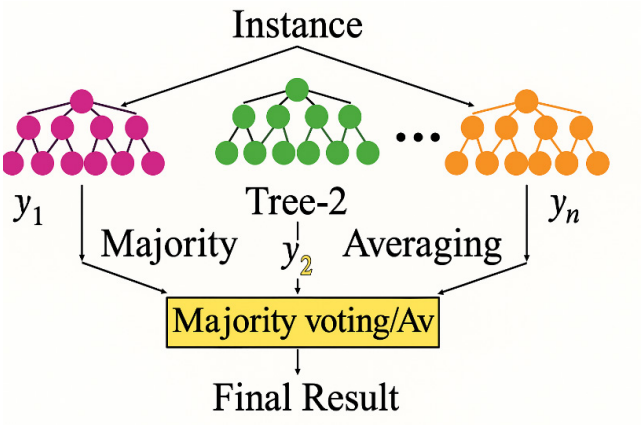


Figure 4. Random forest schematic diagram.

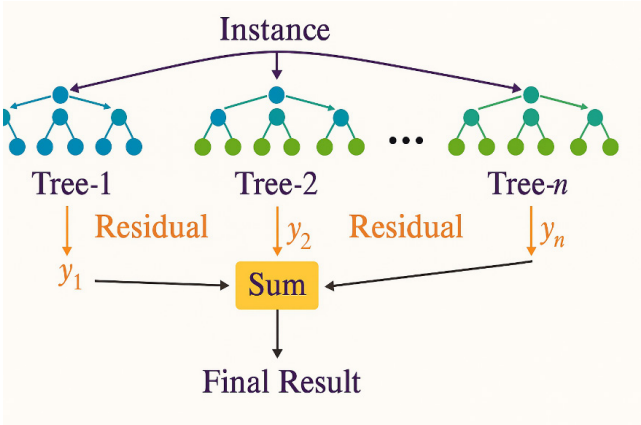


Figure 5. XGBoost schematic diagram.

3.4.2 Extreme Gradient Boosting

The Extreme Gradient Boosting (XGBoost) model, Figure 5, recognised for its superior prediction performance in regression tasks, effectively captures complex nonlinear relationships, handles missing data, and identifies key influencing factors, making it highly suitable for applications like soil pH prediction, arsenic concentration estimation, and liquefaction potential assessment[88-90]. As an ensemble learning method similar to Random Forests, XGBoost requires tuning several hyperparameters, including tree count, depth, regularisation, and learning rate, where Bayesian optimisation, offering greater efficiency over grid search, has been widely employed to achieve globally optimal solutions[91].

The correlation matrix heatmap, Figure 6, provides a comprehensive overview of the interrelationships among the CO_2 test parameters, including Base (B), sample series (S1–S3), and their corresponding PI values. Strong positive correlations are observed between several parameters, such as B and S1 (r = 0.97) and S2 and S3 (r = 0.91), indicating similar trends in their behaviour under CO_2 exposure. In contrast, notable negative correlations are seen between B and S3_PI (r = –0.48) and B and S1_PI (r = –0.34), suggesting inverse relationships between base conditions and plasticity changes in treated samples. The plasticity indices show varied relationships, with S2_PI strongly correlating with S2 (r = 0.72) and S3 (r = 0.74), and S1_PI correlating moderately with S3 (r = 0.49) and strongly with S2_PI (r = 0.70). Further, the heatmap highlighted both direct and inverse interactions among the variables.

The first plot (Unconfined Strength) shows that the RF model effectively captures the general downward trend in strength over increasing exposure, particularly for B, S1, and S3 series, although slight deviations are noted at certain exposure indices, such as S2 around index 2. The second plot (CO_2 Adsorption) demonstrates a clear prediction alignment with actual values across all series, with the RF model accurately reflecting peak adsorption behaviour, notably at exposure index 2 for S2 and S3, and the subsequent decline. This highlights the model's capability to track nonlinear adsorption patterns. The third plot, PI, indicates that the RF model maintains robust predictive accuracy for plasticity trends, particularly for B and S1, though S3 shows some variability between actual and predicted values, especially at early exposure indices.

The RF model showed strong predictive performance across all three parameters, effectively modelling complex patterns and variable interactions over time. This underscores its suitability for capturing the multifaceted behavior of soils under CO_2 exposure, making it a valuable tool for predicting key geotechnical and environmental performance metrics.

Figure 8 illustrates the predictive performance of the XGBoost model for three soil properties—UCS, PI, and CO_2 adsorption—across different samples; B, S1, S2, S3 and exposure indices. The model shows strong alignment between predicted and actual values, indicating effective learning of the underlying patterns in the data. In the case of UCS, the actual and predicted trends for all samples follow a similar pattern, generally showing a decline with increasing exposure index. This suggests that the

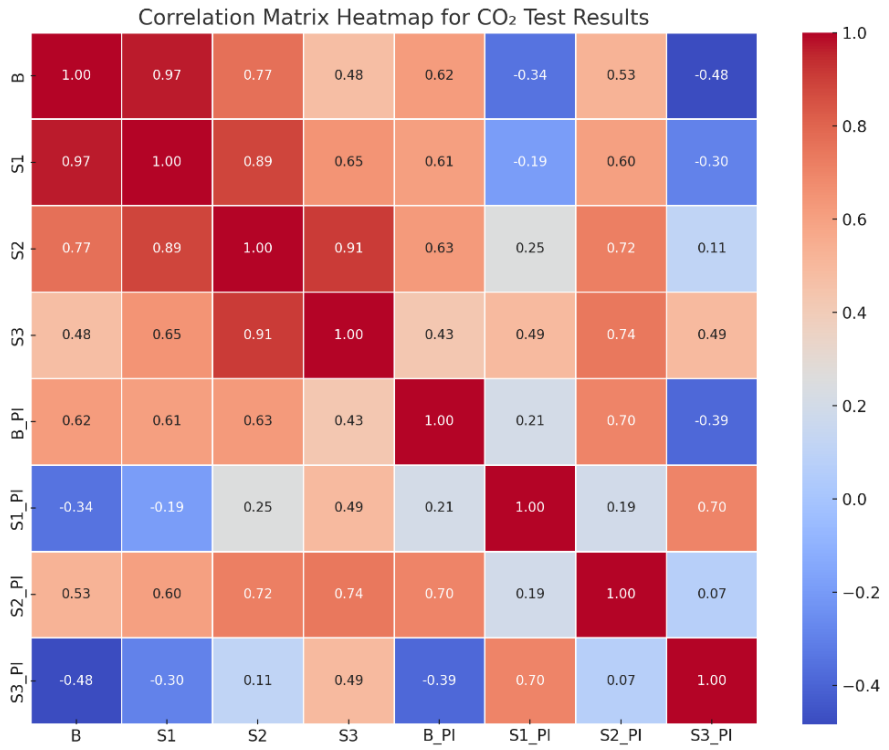


Figure 6. Correlation matrix heatmap.

XGBoost model captures the degradation behavior of the material effectively. However, some discrepancies at certain exposure levels indicate areas where the model may have struggled with more complex or localised behavior, possibly due to insufficient features or slight overfitting.

For the PI, the prediction accuracy is particularly high. The predicted values closely match the actual measurements across all exposure levels and samples, reflecting minimal deviation. This consistency implies that the PI is either more stable or simpler to model, and that the model was well-regularised and trained with a feature set that captured its behavior effectively. The accuracy here highlights XGBoost's ability to model even minor variations with precision, especially in cases where relationships are less complex.

In the case of CO_2 adsorption, the XGBoost model again performs well, accurately tracking changes such as peaks and drops in uptake values across exposure indices. The model successfully captures the nonlinear dynamics and variations in behavior among different samples, which is indicative of its strength in modelling complex interactions and localised changes. The agreement between actual and predicted trends, even during abrupt shifts, demonstrates XGBoost's robustness in handling intricate patterns that could stem from variations in surface chemistry or microstructure due to environmental exposure.

The XGBoost model demonstrates strong predictive capabilities across all three properties, leveraging its strengths in modeling nonlinear relationships and interacting features. While it performs exceptionally well in stable or less complex scenarios like the PI, its minor deviations in strength predictions suggest opportunities for improvement in capturing localised variability, potentially through enhanced feature engineering or additional data.

Figure 9 presents a comparison of prediction errors, measured using Root Mean Square Error (RMSE), for two machine learning models—Random Forest and XGBoost—across various soil-related variables such as unconfined strength, PI, and CO_2 adsorption for different samples, B, S1, S2, and S3. RMSE quantifies the average magnitude of error between predicted and actual values, with lower values indicating more accurate predictions. Visually, the heatmap uses a color gradient from blue

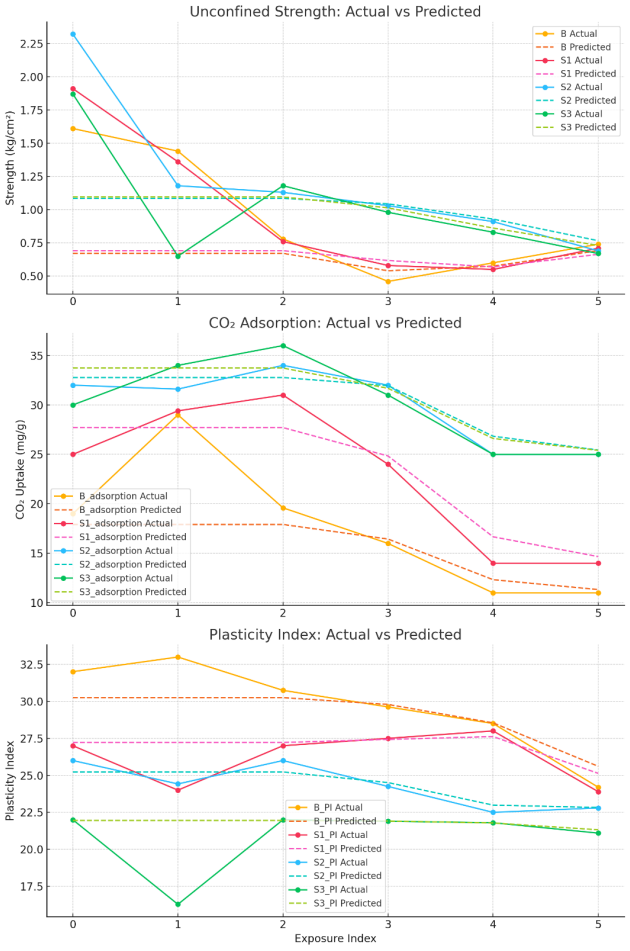


Figure 7. Comparative analysis of actual versus predicted – RF.

(low error) to red (high error) to highlight performance differences between the models.

From the data shown, XGBoost consistently demonstrates superior performance over Random Forest. For instance, in predicting B_adsorption, XGBoost achieves an RMSE of 0.19, whereas Random Forest has a much higher error of 2.05. Similarly, for the PI of sample S3 (S3_PI), Random Forest records an RMSE of 1.17, compared to XGBoost's significantly lower value of 0.08. This trend is observed across all variables and samples, with XGBoost maintaining RMSE values generally below 0.15, indicating strong predictive accuracy and model robustness. These results affirm that XGBoost is better suited for this dataset, likely due to its ability to model complex, nonlinear relationships and its use of regularisation techniques to reduce overfitting. In contrast, Random Forest exhibits larger prediction

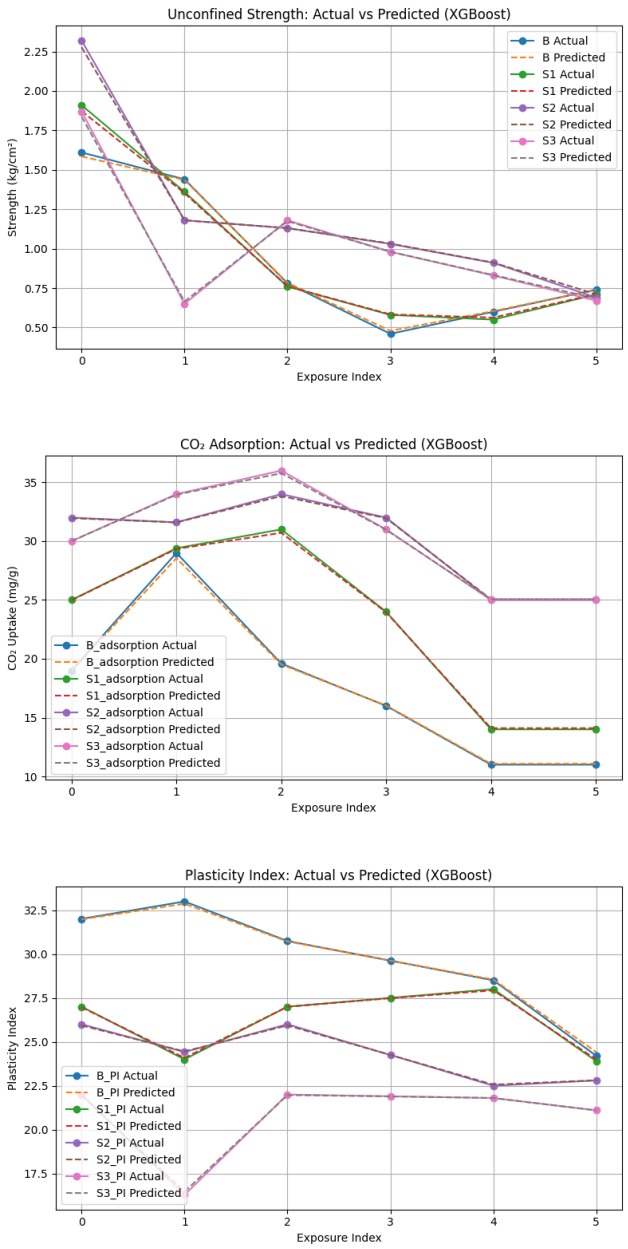


Figure 8. Comparative analysis of actual versus predicted – XGBoost.

errors, particularly for variables with greater variability or complexity, such as CO_2 adsorption and PI. While Random Forest remains a reliable baseline model, its performance in this case is outclassed by XGBoost. Thus, XGBoost is a more effective model for predicting the soil properties examined in this study, offering consistently lower prediction errors and demonstrating greater generalisation capability across all evaluated variables and samples.

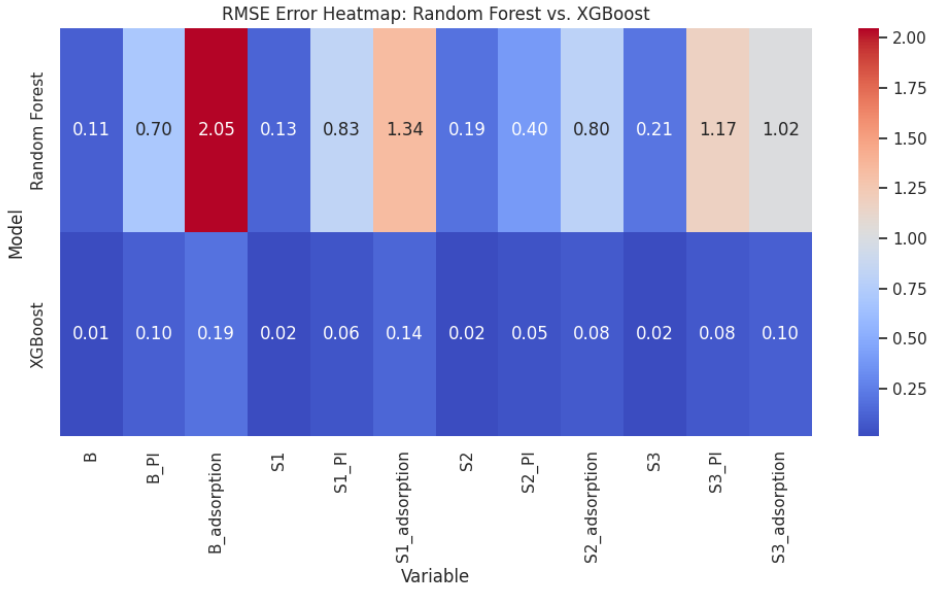


Figure 9. Error metrics heatmap – RF vs XGBoost.

4.0 Conclusions

This study investigated the functionality of GGBS as a stabiliser for expansive soils and a medium for CO_2 sequestration under accelerated carbonation conditions. The key findings are summarised below:

(i) The addition of GGBS significantly improved the unconfined strength of black cotton soil, with 20% GGBS yielding the highest initial strength (2.32 kg/cm²). However, prolonged CO2 exposure led to a gradual decline in strength due to carbonation-induced weakening, followed by partial recovery as stable carbonates formed.

(ii) Plasticity Index decreased across all GGBS-treated samples, with the most pronounced reduction observed in 30% GGBS mixes (PI dropped from 22 to 16.29 within 1 h). This suggests that GGBS not only mitigates swell-shrink behavior but also enhances soil workability over time.

(iii) CO_2 adsorption capacity peaked in 30% GGBS-treated soil (36 mg/g), demonstrating superior carbonation reactivity due to the high calcium oxide content in GGBS. The adsorption trends revealed an initial rapid uptake (peaking at 3–5 h) followed by a gradual decline, indicating saturation of reactive sites. This underscores the potential of GGBS-treated soils as a low-cost, sustainable carbon sink for short- to medium-term CO_2 storage.

(iv) The initial strength reduction under CO_2 exposure was attributed to the formation of weak carbonic acid, which temporarily softened the soil. Subsequent strength recovery (observed in 10% and 30% GGBS mixes) correlated with the precipitation of calcium carbonate ($CaCO_3$), highlighting the dual role of carbonation—both as a destabilising and stabilising process. The latent hydraulic properties of GGBS facilitated long-term strength retention through slow hydration reactions, while its alkaline nature promoted CO_2 mineralisation.

(v) The RMSE heatmap shows that XGBoost consistently achieves lower prediction errors than Random Forest across all variables. It performs especially well in predicting CO_2 adsorption and PI, where Random Forest shows higher deviations. This confirms XGBoost's superior accuracy and suitability for modeling complex soil behavior under CO_2 exposure.

5.0 Authors' Contributions

Sanjeev T P and Muralidhar took care of the conception, methodology, experimental design, data analysis, and overall guidance for the work. Raghavendra HN helped in the literature survey, methodology, and data analysis and assisted in writing and editing. Likhitha H carried out the experimental activity, data collection and validation, and assisted in writing and editing of the manuscript. Arun

Kumar Yadav offered guidance, critical feedback on the results' interpretation, and participated in writing and editing the final manuscript.

6.0 References

1. Nalbantoğlu Z. Effectiveness of class C fly ash as an expansive soil stabilizer. Constr Build Mater. 2004; 18(6):377-381. https://doi.org/10.1016/j.conbuildmat.2004.03.011
2. Nalbantoglu Z, Gucbilmez E. Improvement of calcareous expansive soils in semi-arid environments. J Arid Environ. 2001; 47(4):453-463. https://doi.org/10.1006/jare.2000.0726
3. Mishra AK, Dhawan S, Rao SM. Analysis of swelling and shrinkage behavior of compacted clays. Geotech Geol Eng. 2008; 26:289-298. https://doi.org/10.1007/s10706-007-9165-0
4. Nelson J, Miller DJ. Expansive soils: Problems and practice in foundation and pavement engineering. John Wiley and Sons; 1997.
5. Al-Rawas AA, Taha R, Nelson JD, Al-Shab BT, Al-Siyabi H. A comparative evaluation of various additives used in the stabilization of expansive soils. Geotech Test J. 2002; 25(2):199-209. https://doi.org/10.1520/GTJ11363J
6. Shelke AP, Murty DS. Reduction of swelling pressure of expansive soils using EPS geofoam. Indian Geotechnical Conference; 2010. p. 496-498.
7. Cokca E. Use of class c fly ashes for the stabilizationof an expansive soil. J Geotech Geoenviron Eng. 2001; 127(7):568-573. https://doi.org/10.1061/(ASCE)1090-0241(2001)127:7(568)
8. Ferguson G. Use of self-cementing fly ashes as a soil stabilization agent. Fly ash for soil improvement. Asce Geotechnical Special Publication no. 36; 1993.
9. Kumar BRP, Sharma RS. Effect of fly ash on engineering properties of expansive soils. J Geotech Geoenviron Eng. 2004; 130(7):764-767. https://doi.org/10.1061/(ASCE)1090-0241(2004)130:7(764)
10. Cokca E, Yazici V, Ozaydin V. Stabilization of expansive clays using Granulated Blast Furnace Slag (GBFS) and GBFS-cement. Geotech Geoenviron Eng. 2009; 27:489-499. https://doi.org/10.1007/s10706-008-9250-z
11. Higgins DD. Soil stabilisation with ground granulated blastfurnace slag. UK Cementitious Slag Makers Association (CSMA); 2005.
12. Miller GA, Azad S. Influence of soil type on stabilization with cement kiln dust. Constr Build Mater. 2000; 14(2):89-97. https://doi.org/10.1016/S0950-0618(00)00007-6
13. Zaman M. Soil stabilization using cement kiln dust. Proceedings of the 7th International Conference on Expansive Soils; 1992. p. 1-5.
14. Brooks R, Udoeyo FF, Takkalapelli KV. Geotechnical properties of problem soils stabilized with fly ash and limestone dust in Philadelphia. J Mater Civ Eng. 2011; 23(5):711-716. https://doi.org/10.1061/(ASCE)MT.1943-5533.0000214
15. Wang L. Cementitious stabilization of soils in the presence of sulfate. Louisiana State University and Agricultural and Mechanical College; 2002.
16. Al-Mukhtar M, Lasledj A, Alcover JF. Behaviour and mineralogy changes in lime-treated expansive soil at 20 C. Appl Clay Sci. 2010; 50(2):191-198. https://doi.org/10.1016/j.clay.2010.07.023
17. Bell FG. Lime stabilization of clay minerals and soils. Eng Geol. 1996; 42(4):223-237. https://doi.org/10.1016/0013-7952(96)00028-2
18. Prusinski JR, Bhattacharja S. Effectiveness of Portland cement and lime in stabilizing clay soils. Transp Res Rec. 1999; 1652(1):215-227. https://doi.org/10.3141/1652-28
19. Yong RN, Ouhadi VR. Experimental study on instability of bases on natural and lime/cement-stabilized clayey soils. Appl Clay Sci. 2007; 35(3-4):238-249. https://doi.org/10.1016/j.clay.2006.08.009
20. Chatterjee AK. Indian fly ashes: Their characteristics and potential for mechanochemical activation for enhanced usability. J Mater Civ Eng. 2011; 23(6):783-788. https://doi.org/10.1061/(ASCE)MT.1943-5533.0000279
21. Singh SP, Tripathy DP, Ranjith PG. Performance evaluation of cement stabilized fly ash-GBFS mixes as a highway construction material. Waste Manag. 2008; 28(8):1331-1337. https://doi.org/10.1016/j.wasman.2007.09.017 PMid:18060762
22. Central Electricity Authority (CEA). Report on fly ash generation at coal/lignite based thermal power stations and its utilization in the country for the year 2013-14. New Delhi: CEA; 2013.
23. Sunku JA. Advantages of using fly ash as Supplementary Cementing Material (SCM) in fibre cement sheets. Proceedings of 10th International Inorganic-bonded Fiber Composites Conference; 2006. p. 25-32.
24. Bijen J. Benefits of slag and fly ash. Constr Build Mater. 1996; 10(5):309-314. https://doi.org/10.1016/0950-0618(95)00014-3
25. Pathak AK, Pandey V, Murari K, Singh JP. Soil stabilisation using ground granulated blast furnace slag. Int J Eng Res Appl. 2014; 4:164-171.
26. Rajalaxmi B. Stabilization of red soil using blast furnace slag. Doctoral dissertation.

27. Neeraja D, Rao Narsimha AV. Use of certain admixtures in the construction of pavement on expansive clayey subgrade. Int J Eng Sci Tech. 2010; 2(11):6108-6114.
28. Sridevi G, Sreerama R. Efficacy of GGBS stabilized soil cushions with and without lime in pavements. Int J Emerg Technol Comput Appl Sci. 2014; 9(2).
29. Goodarzi AR, Salimi M. Stabilization treatment of a dispersive clayey soil using granulated blast furnace slag and basic oxygen furnace slag. Appl Clay Sci. 2015; 108:61-69. https://doi.org/10.1016/j.clay.2015.02.024
30. Kavak A, Bilgen G, Capar O. Using ground granulated blast furnace slag with seawater as soil additives in lime-clay stabilization. J ASTM Int. 2011; 8(7):1-12. https://doi.org/10.1520/JAI103648
31. Sargent P. Secondary minerals to replace cement in stabilising an alluvium. Doctoral dissertation, Newcastle University; 2015.
32. Yi Y, Li C, Liu S. Alkali-activated ground-granulated blast furnace slag for stabilization of marine soft clay. J Mater Civ Eng. 2015; 27(4). https://doi.org/10.1061/(ASCE)MT.1943-5533.0001100
33. Yi Y, Liska M, Jin F, Al-Tabbaa A. Mechanism of reactive magnesia-Ground Granulated Blastfurnace Slag (GGBS) soil stabilization. Can Geotech J. 2016; 53(5):773-782. https://doi.org/10.1139/cgj-2015-0183
34. Mohajan HK. Greenhouse gas emissions, global warming and climate change. Proceedings of the 15th Chittagong Conference on Mathematical Physics, Jamal Nazrul Islam Research Centre for Mathematical and Physical Sciences (JNIRCMPS), Chittagong, Bangladesh; 2017.
35. Lead C. Mineral carbonation and industrial uses of carbon dioxide. Carbon Dioxide Capture and Storage. 2005; 10:319.
36. Abedi B, Orujov A, Dabbaghi E, Ng K, Ackerman J, Aryana SA. Containment strategy for subsurface H_2 storage based on time-dependent soft solids. Int J Hydrogen Energy. 2024; 82:1001-1014. https://doi.org/10.1016/j.ijhydene.2024.07.336
37. Peter A, Yang D, Eshiet KI, Sheng Y. A review of the studies on CO_2-brine-rock interaction in geological storage process. Geosciences. 2022; 12(4):168. https://doi.org/10.3390/geosciences12040168
38. Dabbaghi E, Ng K, Kou Z, Copeland G, Alvarado V. Experimental investigation to understand the effect of fracturing fluid on the geomechanical behavior of mowry shale. J Pet Explor Prod Technol. 2024; 14(6):1505-1519. https://doi.org/10.1007/s13202-024-01788-6
39. Pavithra P, Reddy MS, Dinakar P, Rao BH, Satpathy BK, Mohanty AN. A mix design procedure for geopolymer concrete with fly ash. J Clean Prod. 2016; 133:117-125. https://doi.org/10.1016/j.jclepro.2016.05.041
40. Ruan S, Unluer C. Comparative life cycle assessment of reactive MgO and Portland cement production. J Clean Prod. 2016; 137:258-273. https://doi.org/10.1016/j.jclepro.2016.07.071
41. Wang D, Zhu J, He F. CO_2 carbonation-induced improvement in strength and microstructure of reactive MgO-CaO-fly ash-solidified soils. Constr Build Mater. 2019; 229:116914. https://doi.org/10.1016/j.conbuildmat.2019.116914
42. Likhitha H, Raghavendra HN, Rakesh KP, Shrihari UP. Stabilization of sub grade Black Cotton Soil using Cement and M-Sand. International Journal of Engineering Technology Science and Research IJETSR. 2018;5.
43. dos Santos VHJM, Pontin D, Ponzi GGD, e Stepanha ASd, Martel RB, Schütz MK, *et al*. Application of Fourier Transform Infrared Spectroscopy (FTIR) coupled with multivariate regression for calcium carbonate (CaCO3) quantification in cement. Constr Build Mater. 2021; 313:125413. https://doi.org/10.1016/j.conbuildmat.2021.125413
44. Mohammed MA, Yunus NZM, Hezmi MA, Hasbollah DZA, Rashid ASA. Ground improvement and its role in carbon dioxide reduction: A review. Environ Sci Pollut Res Int. 2021; 28:8968-8988. https://doi.org/10.1007/s11356-021-12392-0 PMid:33443736
45. Hu W, Nie Q, Huang B, Su A, Du Y, Shu X, *et al*. Mechanical property and microstructure characteristics of geopolymer stabilized aggregate base. Constr Build Mater. 2018; 191:1120-1127. https://doi.org/10.1016/j.conbuildmat.2018.10.081
46. Lu HY, Lin CK, Lin W, Liou TS, Chen WF, Chang PY. A natural analogue for CO_2 mineral sequestration in Miocene basalt in the Kuanhsi-Chutung area, Northwestern Taiwan. Int J Greenh Gas Con. 2011; 5(5):1329-1338. https://doi.org/10.1016/j.ijggc.2011.05.037
47. Lim M, Han GC, Ahn JW, You KS. Environmental remediation and conversion of carbon dioxide (CO_2) into useful green products by accelerated carbonation technology. Int J Environ Res Public Health. 2010; 7(1):203-228. https://doi.org/10.3390/ijerph7010203 PMid:20195442 PMCid:PMC2819785
48. Huijgen WJ, Ruijg GJ, Comans RN, Witkamp GJ. Energy consumption and net CO_2 sequestration of aqueous mineral carbonation. Ind Eng Chem Res. 2006; 45(26):9184-9194. https://doi.org/10.1021/ie060636k
49. Washbourne CL, Renforth P, Manning DA. Investigating carbonate formation in urban soils as a method for

capture and storage of atmospheric carbon. Sci Total Environ. 2012; 431:166-175. https://doi.org/10.1016/j.scitotenv.2012.05.037 PMid:22683756

50. Papa E, Medri V, Paillard C, Contri B, Murri AN, Vaccari A, Landi E. Geopolymer-hydrotalcite composites for CO_2 capture. J Clean Prod. 2019; 237:117738. https://doi.org/10.1016/j.jclepro.2019.117738
51. Zhou G, Liu S, Li Z, Zhang D, Tang X, Zhou C, *et al*. Old-growth forests can accumulate carbon in soils. Science. 2006; 314(5804):1417. https://doi.org/10.1126/science.1130168 PMid:17138894
52. Manning DA, Renforth P. Passive sequestration of atmospheric CO_2 through coupled plant-mineral reactions in urban soils. Environ Sci Technol. 2013; 47(1):135-141. https://doi.org/10.1021/es301250j PMid:22616942
53. Gough C, Mander S, Haszeldine S. A roadmap for carbon capture and storage in the UK. Int J Greenh Gas Con. 2010; 4(1):1-12. https://doi.org/10.1016/j.ijggc.2009.10.014
54. Zhang X, Fan JL, Wei YM. Technology roadmap study on carbon capture, utilization and storage in China. Energy Policy. 2013; 59:536-550. https://doi.org/10.1016/j.enpol.2013.04.005
55. Lake JA, Johnson I, Cameron DD. Carbon Capture and Storage (CCS) pipeline operating temperature effects on UK soils: The first empirical data. International Journal of Greenhouse Gas Control. 2016 Oct 1;53:11-7.
56. Shepherd JG. Geoengineering the climate: Science, governance and uncertainty. Royal Society; 2009.
57. Milodowski AE, Rochelle CA, Lacinska A, Wagner D. A natural analogue study of CO2-cement interaction: Carbonation of calcium silicate hydrate-bearing rocks from Northern Ireland. Energy Procedia. 2011; 4:5235-5242. https://doi.org/10.1016/j.egypro.2011.02.502
58. Chen YH, Lu DL. CO_2 capture by kaolinite and its adsorption mechanism. Appl Clay Sci. 2015; 104:221-228. https://doi.org/10.1016/j.clay.2014.11.036
59. Cai T, Wang M, Chen X, Wu Y, Ma J, Zhou W. Operando modeling and measurements: Powerful tools for revealing the mechanism of alkali carbonate-based sorbents for CO_2 capture in real conditions. Front Energy. 2023; 17(3):380-389. https://doi.org/10.1007/s11708-023-0872-x
60. Zhang C, Ji Y, Li C, Zhang Y, Sun S, Xu Y, *et al*. The application of biochar for CO_2 capture: Influence of biochar preparation and CO_2 capture reactors. Ind Eng Chem Res. 2023; 62(42):17168-17181. https://doi.org/10.1021/acs.iecr.3c00445 PMid:37900302 PMCid:PMC10603783
61. Malini K, Selvakumar D, Kumar NS. Activated carbon from biomass: Preparation, factors improving basicity and surface properties for enhanced CO_2 capture capacity - A review. J CO2 Util. 2023; 67:102318. https://doi.org/10.1016/j.jcou.2022.102318
62. Alsadi J, Tripathi V, Amaral LS, Potrich E, Hasham SH, Patil PY, *et al*. Architecture fibrous meso-porous silica spheres as enhanced adsorbent for effective capturing for CO_2 gas. Key Eng Mater. 2022; 928:39-44. https://doi.org/10.4028/p-2f2o01
63. Giesting P, Guggenheim S, Van Groos AF, Busch A. Interaction of carbon dioxide with Na-exchanged montmorillonite at pressures to 640 bars: Implications for CO_2 sequestration. Int J Greenh Gas Con. 2012; 8:73-81. https://doi.org/10.1016/j.ijggc.2012.01.011
64. Iglesias I, Jiménez M, Gallardo AM, Ávila EE, Morera V, Viloria A, Ricaurte M, Tafur JP. Mechanical properties and X-ray diffraction analyses of clay/sand pellets for CO_2 adsorption: the effects of sand content and humidity. Oil and Gas Science and Technology–Revue d'IFP Energies nouvelles. 2021; 76:49.
65. Du X, Pang D, Zhao Y, Hou Z, Wang H, Cheng Y. Investigation into the adsorption of CO_2, N_2 and CH_4 on kaolinite clay. Arab J Chem. 2022; 15(3):103665. https://doi.org/10.1016/j.arabjc.2021.103665
66. Heller R, Zoback M. Adsorption of methane and carbon dioxide on gas shale and pure mineral samples. J Unconv Oil Gas Res. 2014; 8:14-24. https://doi.org/10.1016/j.juogr.2014.06.001
67. Kang G, Zhang B, Kang T, Guo J, Zhao G. Effect of pressure and temperature on CO_2/CH_4 competitive adsorption on kaolinite by Monte Carlo simulations. Materials. 2020; 13(12):2851. https://doi.org/10.3390/ma13122851 PMid:32630468 PMCid:PMC7344792
68. Du X, Pang D, Cheng Y, Zhao Y, Hou Z, Liu Z, *et al*. Adsorption of CH_4, N_2, CO_2, and their mixture on montmorillonite with implications for enhanced hydrocarbon extraction by gas injection. Appl Clay Sci. 2021; 210:106160. https://doi.org/10.1016/j.clay.2021.106160
69. Fasihnikoutalab MH, Asadi A, Huat BK, Westgate P, Ball RJ, *et al*. Laboratory-scale model of carbon dioxide deposition for soil stabilisation. J Rock Mech Geotech Eng. 2016; 8(2):178-186. https://doi.org/10.1016/j.jrmge.2015.11.001
70. Fasihnikoutalab MH, Asadi A, Unluer C, Huat BK, Ball RJ, Pourakbar S. Utilization of alkali-activated olivine in soil stabilization and the effect of carbonation on unconfined compressive strength and microstructure. J Mater Civ Eng. 2017; 29(6):06017002. https://doi.org/10.1061/(ASCE)MT.1943-5533.0001833

71. Bureau of Indian Standards. IS 2720 (Part 4): Methods of test for soils - Grain size analysis (Reaffirmed May 2020). New Delhi, India: Bureau of Indian Standards; 1985.
72. Bureau of Indian Standards. IS 2720 (Part 5): Methods of test for soils - Determination of liquid and plastic limit. New Delhi, India: Bureau of Indian Standards; 1985.
73. Chegenizadeh A, Hanson SW, Nikraz H, Scott Kress C. Effects of ground-granulated blast-furnace slag used as filler in dense graded asphalt. Appl Sci. 2022; 12(6):2769. https://doi.org/10.3390/app12062769
74. Collins RJ, Ciesielski SK. Recycling and use of waste materials and by-products in highway construction; 1994.
75. George C, Selvan SS. Integrated analysis of light gauge steel beam sections enhanced by steel fiber reinforced concrete: A comprehensive study on structural and thermal performance. Matéria (Rio de Janeiro). 2024; 29(2):e20230329. https://doi.org/10.1590/1517-7076-rmat-2023-0329
76. George C, Selvan SS. State of Art-Light gauge steel hollow and in-filled columns and beams under elevated temperature. Iran J Sci Technol - Trans Civ Eng. 2023; 47(3):1265-1276. https://doi.org/10.1007/s40996-022-00981-z
77. George C, Selvan SS. Analyzing the structural and thermal behavior of beam sections filled with steel fiber-reinforced concrete in light-gauge steel. Mech Adv Mater Struct. 2025; 32(8):1594-1609. https://doi.org/10.1080/15376494.2024.2367769
78. Saikia A, Baruah D, Das K, Rabha HJ, Dutta A, Saharia A. Predicting compaction characteristics of fine-grained soils in terms of Atterberg limits. Int J Geosynth Ground Eng. 2017; 3:1-9. https://doi.org/10.1007/s40891-017-0096-4
79. Hasnat A, Hasan MM, Islam MR, Alim MA. Prediction of compaction parameters of soil using support vector regression. Curr Trends Civ Struct Eng. 2019; 4(1):1-7. https://doi.org/10.33552/CTCSE.2019.04.000580
80. Zhu P, Zhu Y, Zhang P. Comparison of SVR models for predicting the compaction properties of lateritic soils as novel hybrid methods. Eng Res Express. 2022; 4(3):035038. https://doi.org/10.1088/2631-8695/ac87eb
81. Sinha SK, Wang MC. Artificial neural network prediction models for soil compaction and permeability. Geotech Geol Eng. 2008; 26:47-64. https://doi.org/10.1007/s10706-007-9146-3
82. Khuntia S, Mujtaba H, Patra C, Farooq K, Sivakugan N, Das BM. Prediction of compaction parameters of coarse grained soil using Multivariate Adaptive Regression Splines (MARS). Int J Geotech Eng. 2015; 9(1):79-88. https://doi.org/10.1179/1939787914Y.0000000061
83. Othman K. Deep neural network models for the prediction of the aggregate base course compaction parameters. Designs. 2021; 5(4):78. https://doi.org/10.3390/designs5040078
84. Jalal FE, Xu Y, Iqbal M, Jamhiri B, Javed MF. Predicting the compaction characteristics of expansive soils using two genetic programming-based algorithms. Transp Geotech. 2021; 30:100608. https://doi.org/10.1016/j.trgeo.2021.100608
85. Ardakani A, Kordnaeij A. Soil compaction parameters prediction using GMDH-type neural network and genetic algorithm. Eur J Environ Civ Eng. 2019; 23(4):449-462. https://doi.org/10.1080/19648189.2017.1304269
86. Zhang R, Li Y, Goh AT, Zhang W, Chen Z. Analysis of ground surface settlement in anisotropic clays using extreme gradient boosting and random forest regression models. J Rock Mech Geotech Eng. 2021; 13(6):1478-1484. https://doi.org/10.1016/j.jrmge.2021.08.001
87. Nejad AS, Güler E, Özturan M. Evaluation of liquefaction potential using random forest method and shear wave velocity results. 2018 International Conference on Applied Mathematics and Computational Science (ICAMCS. NET), 2018 Oct 6-8, Hungary: Budapest; 2018. https://doi.org/10.1109/ICAMCS.NET46018.2018.00012
88. Chen T, Guestrin C. Xgboost: A scalable tree boosting system. Proceedings of the 22nd ACM SIGKDD International Conference on Knowledge Discovery and Data Mining; 2016. p. 785-794. https://doi.org/10.1145/2939672.2939785
89. Tziachris P, Aschonitis V, Chatzistathis T, Papadopoulou M, Doukas IJ. Comparing machine learning models and hybrid geostatistical methods using environmental and soil covariates for soil pH prediction. Int J Geo-Inf. 2020; 9(4):276. https://doi.org/10.3390/ijgi9040276
90. Ye M, Zhu L, Li X, Ke Y, Huang Y, Chen B, *et al*. Estimation of the soil arsenic concentration using a geographically weighted XGBoost model based on hyperspectral data. Sci Total Environ. 2023; 858:159798. https://doi.org/10.1016/j.scitotenv.2022.159798 PMid:36309269
91. Zhang W, Wu C, Zhong H, Li Y, Wang L. Prediction of undrained shear strength using extreme gradient boosting and random forest based on Bayesian optimization. Geosci Front. 2021; 12(1):469-477. https://doi.org/10.1016/j.gsf.2020.03.007